Applied Surface Science 525 (2020) 146581

Contents lists available at ScienceDirect

Applied Surface Science

journal homepage: www.elsevier.com/locate/apsusc

Tribological behaviors of in-situ textured DLC films under dry and lubricated conditions

Dongqing He[a,b], Chao He[b], Wensheng Li[a,b,*], Lunling Shang[b,c,*], Liping Wang[a,d], Guangan Zhang[c]

[a] State Key Laboratory of Advanced Processing and Recycling of Nonferrous Metals, Lanzhou University of Technology, Lanzhou 730050, China
[b] School of Materials Science and Engineering, Lanzhou University of Technology, Lanzhou 730050, China
[c] State Key Laboratory of Solid Lubrication, Lanzhou Institute of Chemical Physics, Chinese Academy of Sciences, Lanzhou 730000, China
[d] Key Laboratory of Marine Materials and Related Technologies, Zhejiang Key Laboratory of Marine Materials and Protective Technologies, Ningbo Institute of Materials Technology and Engineering, Chinese Academy of Sciences, Ningbo 315201, China

ARTICLE INFO

Keywords:
DLC films
In-situ texturing
Micro-dimples
Tribological behaviors

ABSTRACT

Surface texturing is emerging as one of the viable means that can be applied to improve the tribological properties of diamond like carbon (DLC) films. In this study, textured DLC films were in-situ fabricated by masking the substrate with metallic meshes during the deposition process. The tribological behaviors of the textured DLC films with micro-dimples densities of 39%, 52% and 58% were studied and compared with that of the un-textured DLC films under dry friction and liquid lubrication conditions. The results showed that the textured DLC films with micro-dimples density of 52% exhibited the lowest average coefficient of friction (COF) and wear rate both under dry friction and liquid lubrication conditions. The improved tribological performance of the textured DLC films with optimum micro-dimples density (52%) under dry friction could be attributed to the friction-induced graphitization of the textured layer and entrapment of wear debris in the micro-dimples. Under liquid lubrication condition, the micro-dimples played the double role of wear debris and lubricating oil reservoirs, then the graphitized textured layer on the worn surface combined with the liquid lubrication film formed a solid-liquid duplex lubricating, thus achieving significantly lower friction and wear.

1. Introduction

Diamond-like carbon (DLC) films have been used in many applications which include automotive components [1], cutting tools [2], computers [3] and other electronic parts [4] and biomedical devices [5] due to their superior mechanical, chemical, electronic, and tribological properties. Despite the fact that DLC films demonstrate far superior properties, the ever-increasing demands of the industry have challenged their performance capabilities, especially their tribological performance [6–9]. To further enhance the tribological performance of DLC films, various attempts have been made, such as elements or compounds doping [10–12], microstructure design [13,14] and surface modification [15,16]. Of all these methods, surface texturing is the one displaying the greatest potential as far as boosting the tribological properties of DLC films is concerned, owing to its simple preparation, remarkable qualities and more affordable processing costs [17,18].

Surface texturing has been proven both theoretical and practically to be a crucial technique to enhance the tribological performance of machine components. In this technique, micro-textures are created on the component surfaces to reduce friction and wear. To achieve these benefits, researchers optimize the geometric parameters of textures, including density, depth, and diameter in particular conditions. The improved tribological performance of textured surfaces could be associated to several mechanisms such as wear debris entrapment for minimizing third body abrasion [19], improvement of hydrodynamic lubrication [20] and load carrying capacity enhancement [21].

The widely used methods to obtain controlled surface texturing can be divided into three groups [22]: high energy beam/electric discharge methods [23], etching techniques [21] and micromachining/forming techniques [24]. As for the texturing of DLC films, there are two ways that can be considered in each method: direct texturing of an already coated part or indirect texturing of a part prior to coating. Amongst the various surface texturing techniques, laser surface texturing (LST) [25] is one of the most widely used thermal energy based noncontact method which can be employed for surface texturing on almost all types of materials. However, the collateral damage during laser material interaction such as multiple spallation of surfaces and material evaporation are inevitable in most LST processes. Thus, application of the LST

* Corresponding authors at: School of Materials Science and Engineering, Lanzhou University of Technology, Lanzhou 730050, China.
E-mail addresses: liws@lut.edu.cn (W. Li), shangll@licp.cas.cn (L. Shang).

https://doi.org/10.1016/j.apsusc.2020.146581
Received 13 January 2020; Received in revised form 15 March 2020; Accepted 3 May 2020
Available online 06 May 2020
0169-4332/

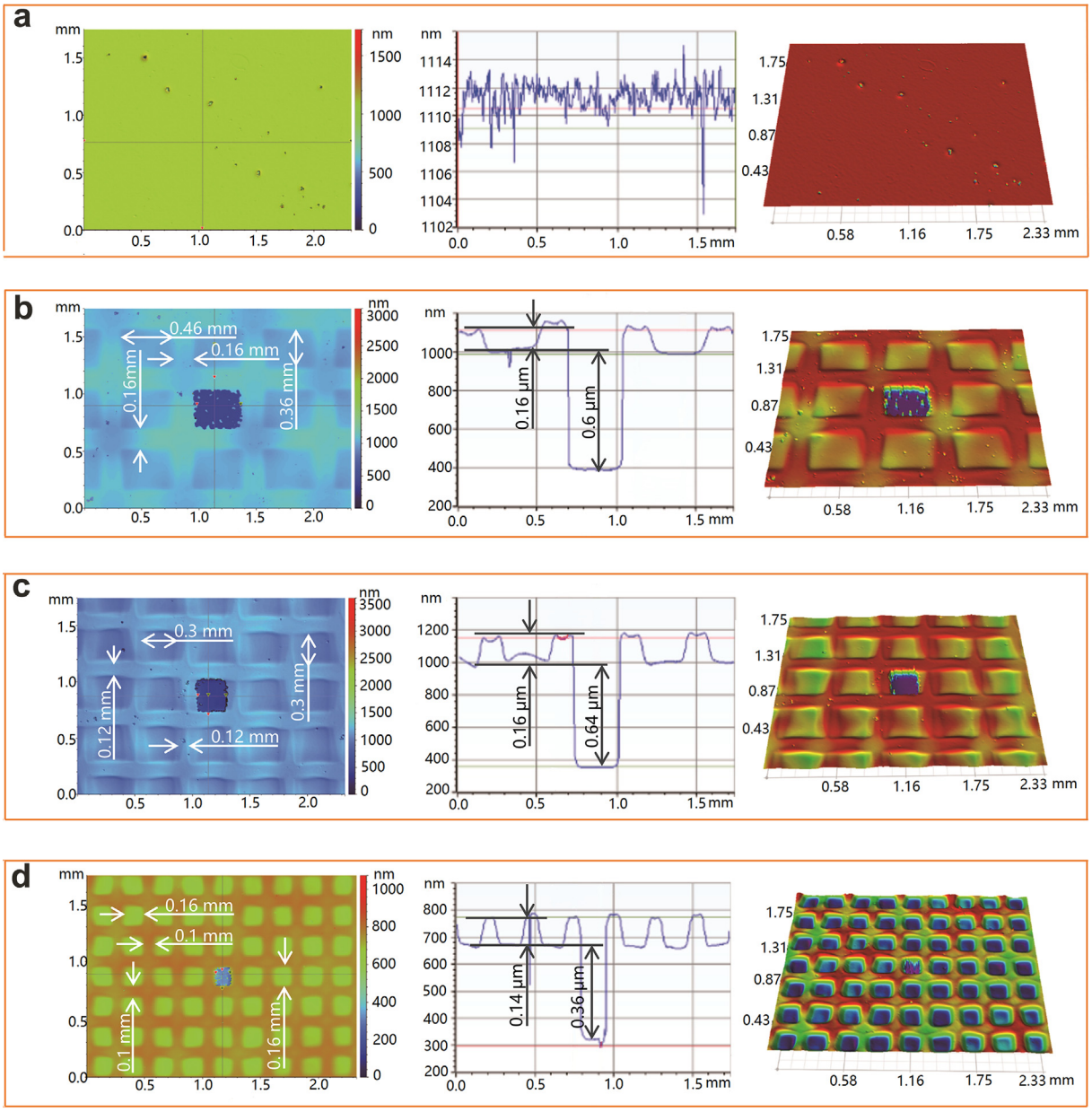

Fig. 1. The surface 2D/3D images and dimples depth profile of DLC-smooth (a), DLC-T39% (b), DLC-T52% (c) and DLC-T58% (d).

technique is still restricted in cases of direct or indirect film texturing given that comprises risks of collateral damages on film or substrate.

In the present study, the micro-textured DLC films were in-situ deposited by masking the substrate with metallic meshes during the deposition process, and the focus of this study is the tribological behaviors of the in-situ textured DLC films under dry and lubricated conditions. The tribological properties of the in-situ textured DLC films with various texture densities and un-textured DLC films were contrastively studied, and the friction-induced material evolution on the sliding surface was investigated. Based on these studies, the effect of the texture size, relevant friction and wear mechanism under dry friction and liquid lubrication conditions were revealed in detail.

2. Experimental

2.1. In-situ deposition of textured DLC films

Depositions were carried out in a closed field unbalanced magnetron sputtering (CFUBMS) system with two graphite targets and two Cr targets. The polished (Ra $\leq$ 0.03 μm) AISI 316 stainless steel sheets (30 mm × 30 mm × 10 mm) and Si (1 0 0) wafers were selected as substrates. Prior to film deposition, the substrates were ultrasonically degreased with acetone and methanol for 10 mins and then cleaned with Ar^+ ions for 20 min at a substrate pulsed bias of −500 V to remove surface oxide and trigger surface activation. A thin Cr adhesion layer (~200 nm) and a Cr → C graded interlayer (~100 nm) were deposited to improve the adhesion of the DLC films. In order to obtain micro-textured DLC films, metallic meshes with different grid intervals of 0.16 mm, 0.3 mm and 0.46 mm were placed on the substrate surface during the film deposition process. According to our previous experiments, if the metallic meshes were tightly covered on the substrate surface, the final deposited DLC films will be divided into discrete pieces because there was no film at all in the place covered by the metallic meshes. Thus, the overall strength, load-bearing capacity, wear resistance and corrosion resistance of the DLC films would be greatly reduced. Therefore, to obtain continuous and full covered DLC films with a top texture layer, the metallic meshes were not tightly covered on the substrate surface, but maintained at a certain distance, and this

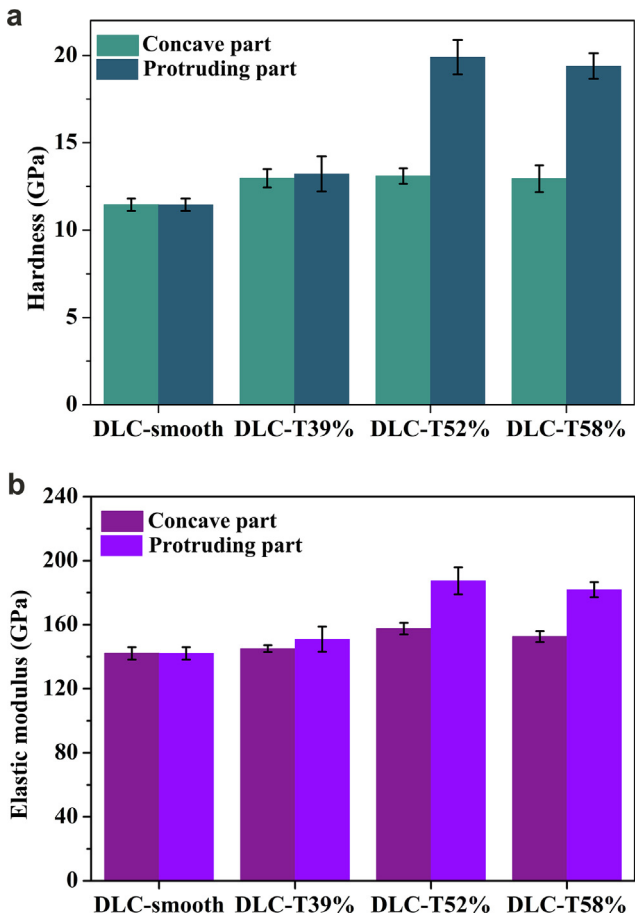

Fig. 2. The hardness (a) and elastic modulus (b) of concave and protruding part of textured DLC films.

distance was strictly controlled between 50 and 200 μm. Then, both textured and un-textured DLC films with thickness averages from 0.5 to 0.8 μm were deposited by sputtering of high-purity graphite targets at a DC power supply of 2500 W. The film deposition was started at a pressure of around 3×10^{-3} Pa and the deposition process was carried out at substrate pulsed bias of −70 V, frequency of 250 kHz and process pressure of 0.2 Pa under Ar flow. The obtained samples were labeled with their texture density: DLC-smooth, DLC-T39%, DLC-T52%, and DLC-T58%.

2.2. Tribological evaluation

Tribological tests were performed on a CSM tribometer in ball-on-disk reciprocating mode with amplitude of 5 mm and sliding frequency of 5 Hz under dry and liquid lubricating conditions at 25 °C. The load applied for dry and lubricated tests were 10 N and 20 N, respectively. The theoretical minimum of the initial Hertzian contact stress was about 1.22 GPa under dry friction and 1.53 GPa under lubricated condition according to the ball-disk (un-textured plane) contact mode. The AISI52100 steel ball with a diameter of 6 mm was used as the friction counterpart. Before tribological tests, specimens and balls were cleaned with ethanol to make sure there were no residual and solid contaminants on sample surfaces. The lubricating oil used in liquid lubricant condition tests was Poly alpha olefins (PAO 8), which was dripped onto the sample surface with a fixed quantity to provide a continuous lubricant film between the steel balls and DLC films. After friction testing, the sliding balls were observed by scanning electron microscopy (SEM) or optical microscopy (OM) and the wear tracks were observed by an optical profiler (Micro XAM 3D). Eventually, the average wear volume could be obtained by measuring each wear track in the cross for three times. Hence, the specific wear rate was calculated as the ratio of the wear volume loss over the normal load multiplied by the total reciprocating sliding distance. The micro-Raman spectroscopy equipped with a 532 nm argon ion laser from 600 to 2000 cm^{-1} was used to investigate the structural properties of the DLC films before and after friction testing.

3. Results and discussion

3.1. Characterization of the textured DLC films

Fig. 1 shows the surface images of micro-textured DLC films with different geometric dimensioning. The micro-dimples area densities of textured DLC films are 39%, 52% and 58% (Fig. 1b–d). The mean area density is calculated by the ratio of the micro-dimples area to the total area. As shown in Fig. 1b, the micro-dimple width and length of the DLC-T39% were 0.46 and 0.36 mm, respectively, and the interval between these two dimples was 0.16 mm. The other two samples (DLC-T52% and DLC-T58%) had a common feature, which was that the width and length of their micro-dimples were the same, and the values were 0.3 mm (Fig. 1c) and 0.16 mm (Fig. 1d), respectively. The micro-dimples interval of these two samples were 0.12 mm and 0.1 mm. Fig. 1 also presents the 2D micro-dimple depth profile, the total thickness of the three textured DLC films were 0.76 μm, 0.8 μm and 0.5 μm, and the depths of the dimples were 0.16 mm, 0.16 mm and 0.14 mm, respectively. The topographic features of micro-dimples were more obvious in 3D images of the textured samples, but unexpectedly the covered region became the concave part while the exposed region became the protruding part. This phenomenon may account for the micro-clearance between the metal mesh and the substrate. During the deposition process, many of the sputtering species remained in a natural state, and as a result, they could not be controlled by the electric and magnetic fields proposed by Nakao et al [26]. While the presence of metal meshes would affect the distribution of the sputtering species, and the density around the wire increased, thus increasing the deposition rate of the DLC films under the metal meshes. This meant that the depth of the texture dimples depended on the height of the protruding part of the textured layer. The experimental results revealed that in a certain range (50–200 μm), the larger the clearance, the faster the deposition rate increases. Therefore, the depth of the texture dimples could be controlled by strictly regulating the clearance distance between the metal meshes and the substrate surface.

Hardness and elastic modulus of the textured and un-textured DLC films were determined using a nanoindenter with a load of 10 mN. Fig. 2 illustrates the variation of hardness (Fig. 2a) and elastic modulus (Fig. 2b) on the concave and protruding parts of the textured DLC films. It could be seen that hardness and elastic modulus of the un-textured DLC films were lower than those of the textured samples. In addition, the hardness and elastic modulus indicated the same trends that the value of the concave part was lower than that of the protruding part and they were increasing at first and then dropped later on. The hardness of the concave and protruding part shown in Fig. 2a increased from about 11 GPa at DLC-smooth to maximum values of about 13 GPa and 19 GPa at DLC-T52%, respectively. An interesting fact was that when the micro-dimples density was up to 52% the hardness of the protruding part of the textured DLC films was much higher than that of the concave part. The elastic modulus of the concave and protruding parts in Fig. 2b rose to about 157 GPa and 187 GPa at DLC-T52%, respectively, and then declined to approximately 152 GPa and 181 GPa at DLC-T58%, indicating that surface texturing was helpful in improving the hardness and elastic modulus of the DLC films.

Raman spectroscopy is widely used to investigate detailed structural feature of DLC films. The prime interest in the DLC films is to probe the sp^3 content which played a significant role on the properties of the films. The Raman spectra of un-textured and textured samples is

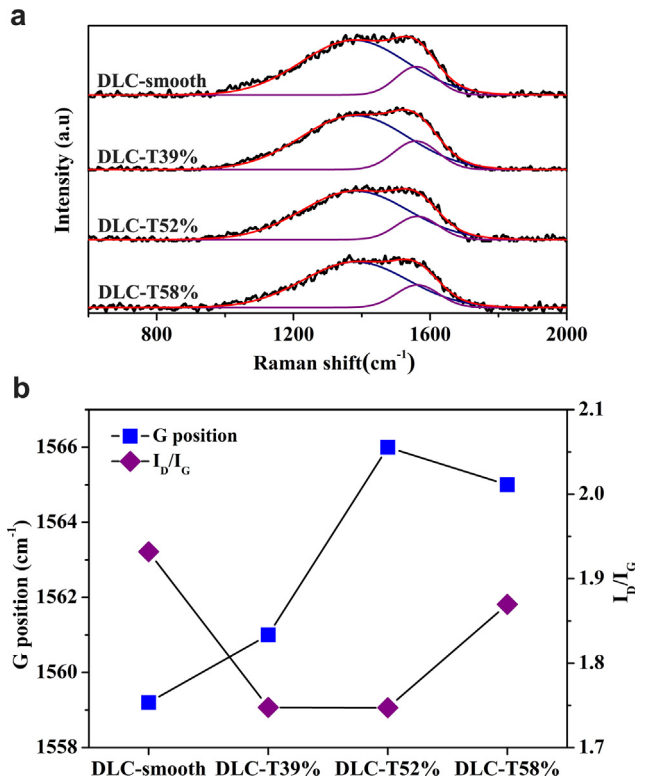

Fig. 3. Raman spectra of the DLC films (a) and the corresponding I_D/I_G and G position (b).

presented in Fig. 3a. A broad peak appeared in the frequency ranging from 600 to 2000 cm^{-1}. As observed, these samples showed a typical DLC shoulder (D-peak around 1380 cm^{-1}) on a skewed broad peak (G-peak around 1560 cm^{-1}). Fig. 3b illustrates the intensity ratio of D peak to G peak (I_D/I_G) and G positions as a function of the dimples density. The I_D/I_G decreased first and then increased afterwards with increase of the dimples density while the G peak positions remained almost unchanged, which implied that the textured DLC films contain relatively higher sp^3 bonded carbon compared with un-textured DLC films. Meanwhile the increased I_D/I_G at DLC-T58% indicated that an excessively high texture density was not conducive to increasing the sp^3 content [27]. This tendency agreed well with the changes of hardness and elastic modulus of textured and un-textured samples.

Contact angle measurements were carried out to investigate the lipophilicity of the textured and un-textured samples, and the final contact angle was determined by averaging values at five different points on each sample surface. Values of samples' contact angles were presented in Fig. 4. It could be seen that the oil contact angles of textured samples were lower than that of un-textured sample. The smaller the contact angle, the better the lipophilicity. Thus, among the textured samples, the specimens with dimples density of 52% exhibited super lipophilicity due to the lowest contact angle about 23.5°. The lipophilic DLC coating surface usually had a high surface energy and it would provide a much stronger interaction between the oil and the DLC surface, suggesting a continuous lubricant film with high adhesiveness to the DLC surface during the sliding process under oil lubrication [28].

3.2. Tribological properties

3.2.1. Dry friction

Fig. 5 shows the coefficient of friction (COF) and wear rates of the DLC films as a function of reciprocating sliding time, and the average COF in steady state is also provided in the inset illustration. According to Fig. 5a, after a short run-in period, the COF of all textured specimens

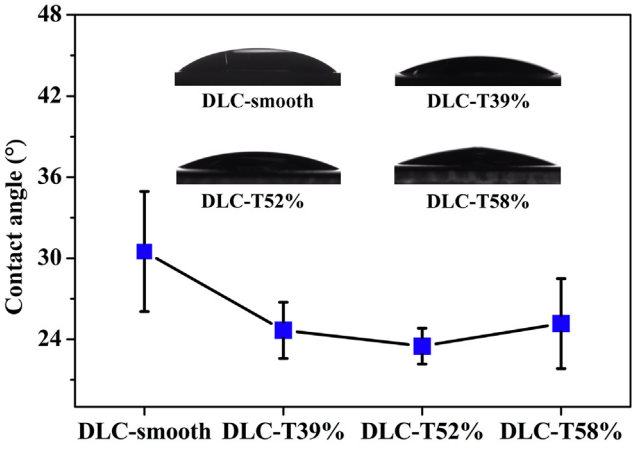

Fig. 4. The contact angle of textured and un-textured DLC films.

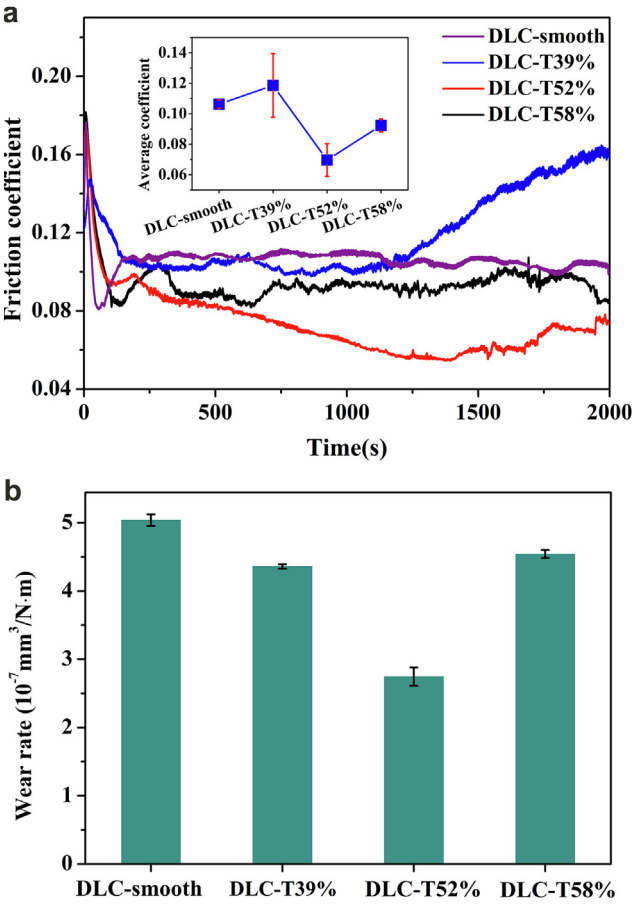

Fig. 5. Friction coefficients (a) and wear rates (b) of textured and un-textured DLC films under dry friction condition.

were smaller than that of un-textured one. After a sliding time of 1250 s, the COF of DLC-T39% increased initially and exceeded un-textured sample. While for the other textured samples, the COF was always smaller than that of the un-textured sample, even the COF of DLC-T52% continued to decrease to a minimum value of about 0.05 after the run-in period. The decreased COF of the textured specimens might be attributed to the friction induced optimization of the textured sliding surface (graphitization and wear debris entrapment), and this shall be further discussed in the following section. Fig. 5b illustrates the wear rates of all the specimens. It was pretty obvious that the wear rates of textured specimens were lower than un-textured one. Remarkably,

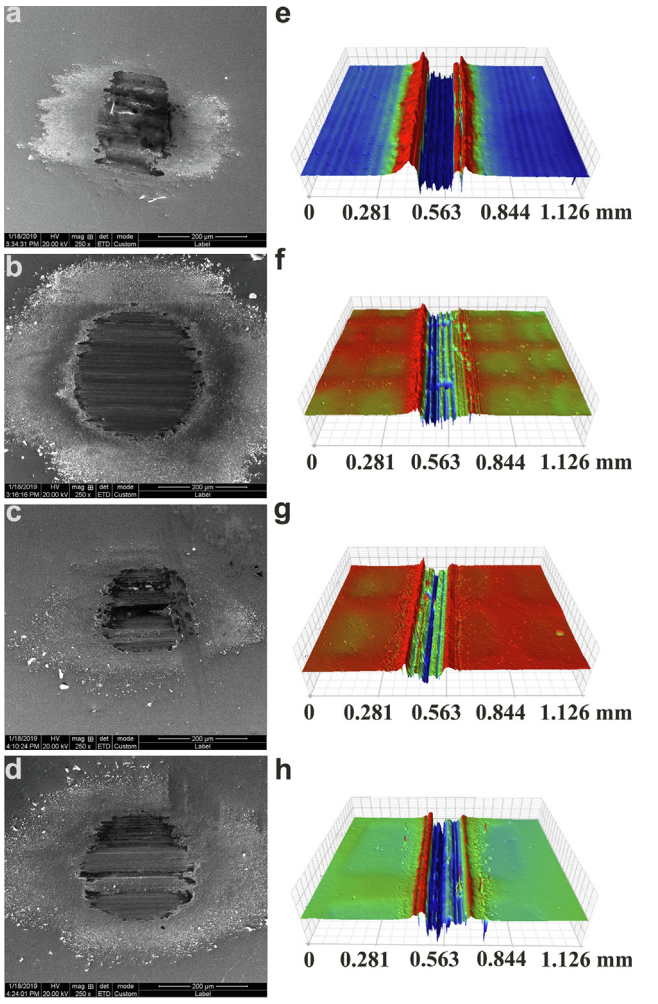

Fig. 6. The SEM images of worn ball surfaces and the corresponding 3D images of wear tracks under dry friction condition: DLC-smooth (a/e), DLC-T39% (b/f), DLC-T52% (c/g) and DLC-T58% (d/h).

DLC-T52% exhibited a superior anti-wear property and showed the lowest wear rate. The anti-wear performance of these DLC films was highly consistent with their hardness, elastic modulus and COF.

Fig. 6 shows the SEM images of the worn ball surfaces and the 3D images of the wear tracks on DLC films. Transfer film formation was clearly observed on the wear scars, especially for the one sliding against the un-textured DLC film, DLC-T52% and DLC-T58%. For DLC films, the formation of transfer film involves two important processes: graphitization and transfer. Surface texturing with appropriate dimples density promoted graphitization of the sliding surface due to the increased contact stress caused by the decreased real contact area. The sharp edges of texture dimples constantly scratched the sliding surface during the sliding process, resulting in the continuous transfer of the graphitized film to the coupled steel ball surface and distributing them along the sliding direction, thus the transfer film on the steel balls sliding against the textured specimens presented obvious directionality (Fig. 6b–d). A continuous and compacted transfer film has been proved to prevent the direct contact between friction pairs effectively, then resulting in low COF and wear [29]. In addition, the wear scar sliding against the DLC-T52% showed the minimum size indicating the smallest contact area, thus further reducing COF. However, the steel ball sliding against the DLC-T39% revealed an abnormally large wear scar indicating a severe wear of the steel ball. This might be due to the low dimples density. The lower the dimples density, the larger the texture's dimple size. Thus, the contact surface of the steel ball would be caught in the large dimples and be continuously cut by the dimple's edge during the sliding process eventually resulting in an ever-increasing contact area and COF. The 3D images of wear tracks (Fig. 5e–h) presented that the wear depth and width decreased initially and then increased and both finally reached the minimum at DLC-T52%. It was worth noting that there was a large amount of accumulated wear debris around the wear track of untextured DLC film, while there was only a small amount of wear debris for the textured one. This meant that the textured dimples could effectively capture the wear debris and store them. It has been proven that the accumulation of the wear debris in the direction of sliding strongly affects the deviation and stability of the tribological performance [17]. Once the wear debris captured in the dimples were rolled repeatedly to form a compacted smooth tribofilm during the sliding process, the friction and wear of the DLC film would be reduced significantly. While for the DLC-T39%, the amount of wear debris caused by the severe wear of the steel ball exceeded the storage capacity of the textured dimples, thus some wear particles were transferred to the steel ball side (Fig. 6b).

Furthermore, with investigation of the phase transformation of DLC films during the friction test as sole objective, a micro-Raman spectroscopy was performed so as to acquire information about the arrangement and alignment of the carbonaceous network. Fig. 7 displays the Raman spectra obtained from the wear tracks under dry friction condition (Fig. 7a) and the corresponding I_D/I_G ratio and G peak position (Fig. 7b). Two shoulders at 1381–1385 cm^{-1} and 1561–1571 cm^{-1} can be observed on the Raman spectra, corresponding to D band and G band respectively. Table 1 lists the Gaussian fitting results of Raman spectra of as-deposited films in Fig. 3a and the wear tracks of textured and un-textured DLC films in Fig. 7a. Compared with the as-deposited DLC films, G peak position of wear track of DLC-smooth and DLC-39% increased by 10 cm^{-1}, respectively. Nevertheless, the G peak position of DLC-39% and DLC-58% in the wear track were almost the same to the as-deposited film. The I_D/I_G ratio in the wear track of the DLC-T52% increased from 1.75 to 2.0 compared with

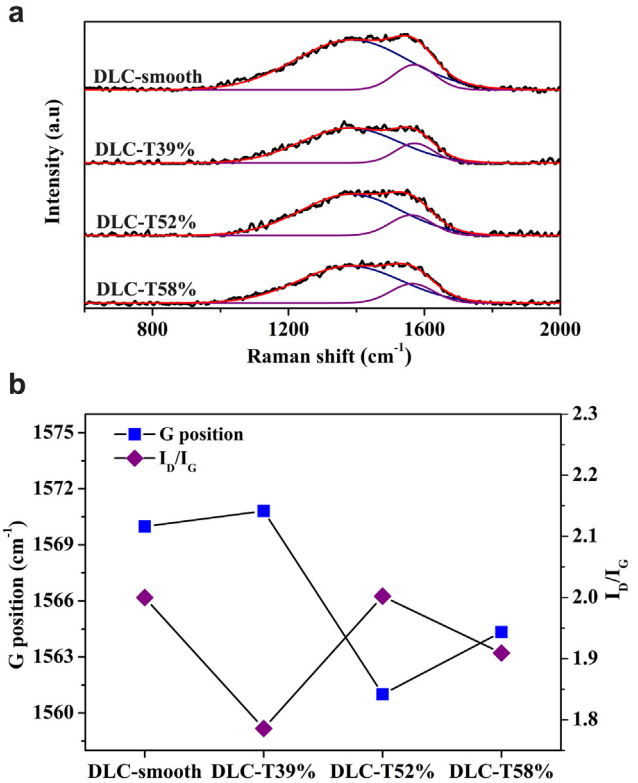

Fig. 7. Raman spectra of wear tracks (a) and the corresponding I_D/I_G and G peak position (b) under dry friction condition.

Table 1
The fitting results of Raman spectra in Figs. 3 and 7a.

Samples		D peak position (cm^{-1})	G peak position (cm^{-1})	I_D/I_G
DLC-smooth	As-deposited	1377	1559	1.93
	Wear track	1385	1569	2.00
DLC-T39%	As-deposited	1382	1561	1.75
	Wear track	1380	1571	1.78
DLC-T52%	As-deposited	1383	1566	1.75
	Wear track	1383	1561	2.00
DLC-T58%	As-deposited	1384	1565	1.87
	Wear track	1381	1564	1.91

the as-deposited film, while the I_D/I_G ratio for the other samples slightly changed. According to Ferrari and Robertson's [30,31] three-stage model about the Raman spectra of disordered and amorphous carbon, the DLC-T52% underwent an obvious graphitization process during the friction testing. Some of the graphitized tribofilm was transferred to the steel ball surface by the sliding process, thus the real sliding interface was changed from between DLC and steel ball to graphitized tribofilm and graphitized transfer film. The low shear property of internal sliding of this graphitized carbon material resulted in a low COF, and the repeated transfer of the graphitized carbon between the two sides of the sliding surfaces prevented any severe wear of the friction pairs [32].

It could be seen from the 3D images of the wear tracks shown in Fig. 6e-h that the wear depth had exceeded the micro-dimples depth at the end of the friction test. That is, surface texturing may only play a role at the early stages of the friction process. Fig. 8 illustrates the initial contact state of un-textured and textured DLC films during the friction test. As shown in Fig. 8a, for the un-textured DLC films, amounts of wear particles stacked at the interface interfered with the sliding process and caused some severe abrasive wear. Additionally, high contact pressure casused by the wear particles lowered the graphitization temperature and thus triggered the graphitization transformation [15], which increased adhensive wear due to the graphitization caused softening of the sliding surfaces. During the friction process, the graphitized layer was continually transferred to the steel ball surface to form a compacted and dense transfer film (Fig. 6a), thus the worn film surface still presented the initial structural characteristics of diamond-like carbon (Fig. 7). As for DLC-T52%, it also underwent an obvious graphitization transformation because of the high contact stress caused by the decreased contact area. However, unlike the un-textured DLC films, although material transfer still occurred on the sliding surface, most of the graphitized wear debris were trapped by the micro-dimples during the sliding process as shown in Fig. 8b. Therefore, DLC-T52% simultaneously achieving low friction and wear due to the interfacial sliding between the graphitized tribofilm and transfer film. According to the tribological features of DLC films [6,29,33], once a stable low-friction interface is formed, the graphitized carbon will be transferred repeatedly between the two sides of the sliding surfaces rather than causing severe wear of the friction pairs. Therefore, even the texture layer was worn through (Fig. 6g), the friction coefficient did not change significantly (Fig. 5a). So from the experimental presentations, the surface texture layer only played a role in the early stage of friction process, but from the tribological mechanism, it laid the foundation for achieving and keeping the low friction. However, when the micro-dimples densities were smaller, such as in DLC-39% (Fig. 8c), the steel ball was easy to sink into the larger dimples, which resulted in the increase of the sliding resistance and plough-cutting of contact surface. As a result, the real contact area was constantly extended, and hence increasing the friction coefficient. Meanwhile when the micro-dimples densities were too large, such as DLC-58% (Fig. 8d), the framework of the textured layer was too thin, thus the textured layer was easily worn out during the slding process and failed to function as the textured layer in DLC-T52%.

3.2.2. Liquid lubrication

To study the impact of in-situ texturing on the tribological behaviors of DLC films under liquid lubrication, a certain amount of PAO 8 oil was added to the sliding interface of the friction pairs. The COF of textured and un-textured samples are shown in Fig. 9a. Under liquid lubrication condition, the COF of the un-textured sample was higher than that of the textured samples and the frictional coefficient curves of textured samples were more stable and smoother than that of DLC-smooth. The illustrated average COF showed that the textured samples exhibited almost the same friction coefficient of 0.075–0.077. The wear rates of the textured and un-textured DLC films are presented in Fig. 9b. The textured DLC films showed a significant lower wear rate compared with the DLC-smooth. Whilst among the textured samples, DLC-52% showed outstanding low wear rate indicating a superior wear resistance. Thus, in-situ surface texturing can effectively improve the tribological performance of DLC film not only under dry friction but also under liquid lubrication condition.

The OM images of the worn ball surfaces sliding against the textured and un-textured DLC films are displayed in Fig. 10a–d. It was obvious that the wear scars on the steel balls sliding against the textured DLC films were smaller than the one sliding against the un-textured film. When the micro-dimples density was 52%, the steel ball was significantly less worn out. The 3D topographies of the wear tracks are illustrated in Fig. 10e–h. A series of furrows on the worn surface of DLC-smooth indicated a severe abrasive wear, and an amount of scratches on the corresponding worn ball surface (Fig. 10a) further confirmed this. The wear tracks of the textured DLC film were smoother and narrower than that of the DLC-smooth, especially the DLC-52%. Under liquid

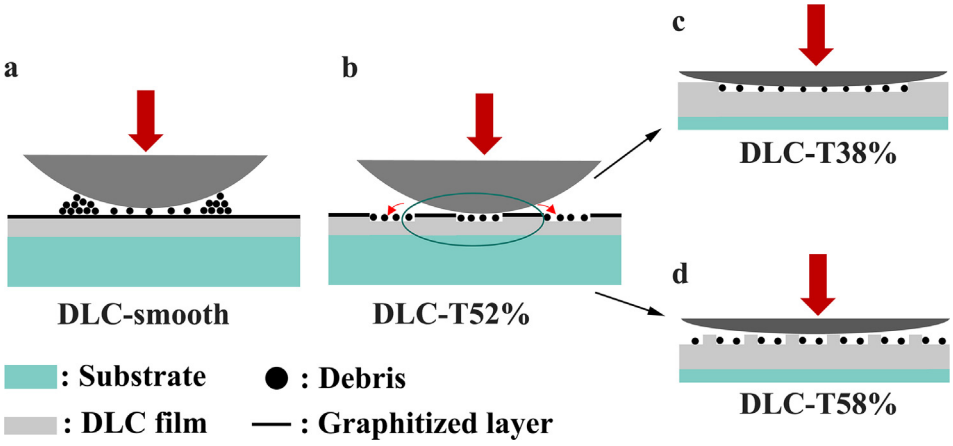

Fig. 8. Schematic illustration of friction and wear mechanism for DLC-smooth (a), DLC-T52% (b), DLC-T38% (c) and DLC-T58% (d) under dry friction condition.

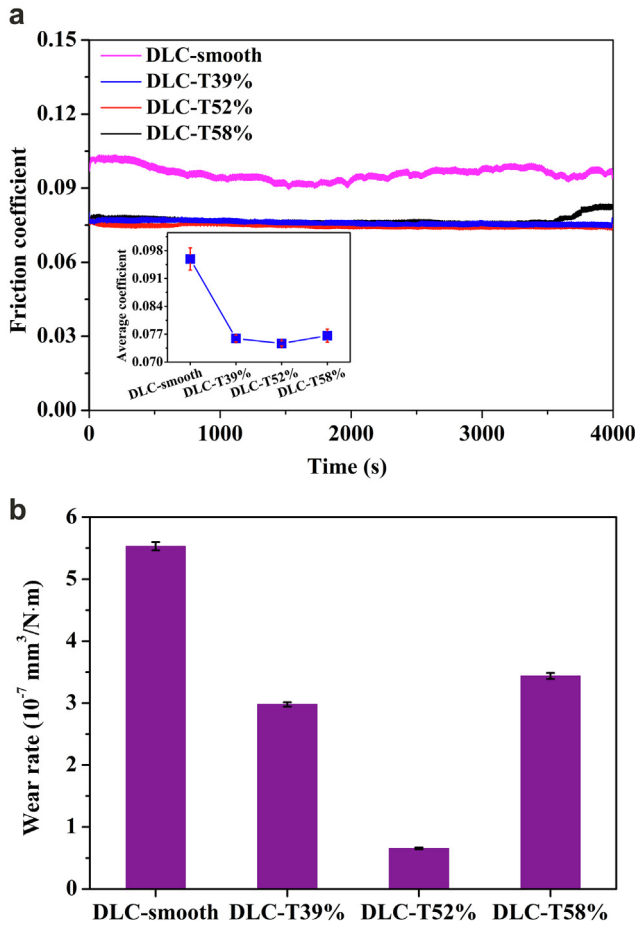

Fig. 9. Friction coefficients (a) and wear rates (b) of textured and un-textured DLC films under liquid lubrication condition.

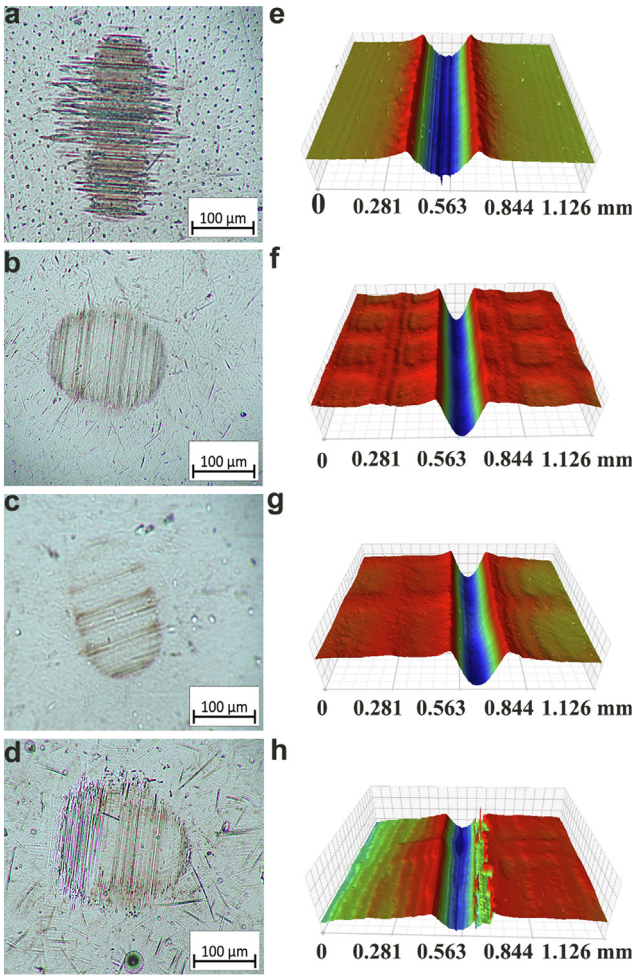

Fig. 10. Optical microscope images of worn ball surfaces and the corresponding 3D images of wear tracks under liquid lubrication condition: DLC-smooth (a/e), DLC-T39% (b/f), DLC-T52% (c/g) and DLC-T58% (d/h).

lubrication condition, the improved tribological properties of the textured DLC film might be attributed to the dual function of wear debris capturing and oil storage in micro-dimples. As observed in Fig. 4, surface texturing considerably decreased the contact angle between PAO and DLC film, which in turn increased its lipophilicity and promoted the formation of thick and continuous lubricating films on the sliding interface, thus resulting in lower friction and wear [34].

The Raman spectra of the wear tracks and the corresponding I_D/I_G ratio and G peak positions under liquid lubrication condition are presented in Fig. 11. The Gaussian fitting results of the as-deposited film's Raman spectra and the wear tracks are shown in Table 2. It could be seen that the I_D/I_G ratio of wear tracks of the textured samples was higher than that of the un-textured sample. For the DLC-smooth, the G peak position shifted from 1559 to 1572 cm^{-1} after the friction test, while the I_D/I_G was almost unchanged. For the textured samples, there was no significant difference in the D peak and G peak positions in-between the as-deposited films and wear tracks. However, compared to the as-deposited film, the I_D/I_G ratio of the wear track of DLC-39%, DLC-52% and DLC-T58% sharply increased from 1.75 to 2.07, 1.75 to 2.03 and 1.87 to 2.0, respectively. These results indicated that the textured samples clearly underwent more significant graphitization than DLC-smooth during the friction test, particularly those of DLC-39% and DLC-T52%. To make it easier for evaluation the friction and wear behavior of DLC films under liquid lubrication condition, the applied load and friction test duration were deliberately increased; the applied load was 20 N and the friction test duration was 60 min. Under such harsh conditions, friction-induced graphitization of DLC film was inevitable, especially for the textured DLC film due to the increased contact pressure caused by the decreased contact area.

Fig. 12 illustrates the schematic view of the sliding contact state for the textured and un-textured DLC films under liquid lubrication condition. For the un-textured specimen shown in Fig. 12a, the wear debris were randomly dispersed to all the sliding interfaces along with the flow of the lubricating oil, thus interfering with the sliding process and accelerating abrasive wear. On the other hand, even the DLC film had been graphitized under heavy load (20 N), the graphitized layer was also washed away by lubricating oil, which made it difficult to achieve a solid–liquid duplex lubrication effect and was also the reason why the Raman signal of graphitization in the wear track of DLC-smooth was less significant. While for the textured DLC films shown in Fig. 12b, micro-dimples could serve as reservoirs for wear debris and lubricating oil. The graphitized wear debris were stored in the micro-dimples and continuously compacted to a dense graphitized layer during the sliding process. Consequently, the graphitized layer on the worn surface combined with the liquid lubrication film resulted in a solid-liquid duplex lubrication effect. Even if the textured layer was worn through, the micro-dimples from outside the contact region could still trap wear debris and store oil. Nonetheless, the function of the wear debris/oil reservoirs and the real contact pressure competed during boundary lubrication sliding [35]. When the dimple density was too low (DLC-T39%), the wear debris could not be totally captured in the micro-dimples and the stored oil was not sufficient to form a thick lubrication film on the sliding interface. On the other hand if the dimple density was excessively large (DLC-T58%), the decreased contact area would increase the average contact stress on the sliding surface and thus

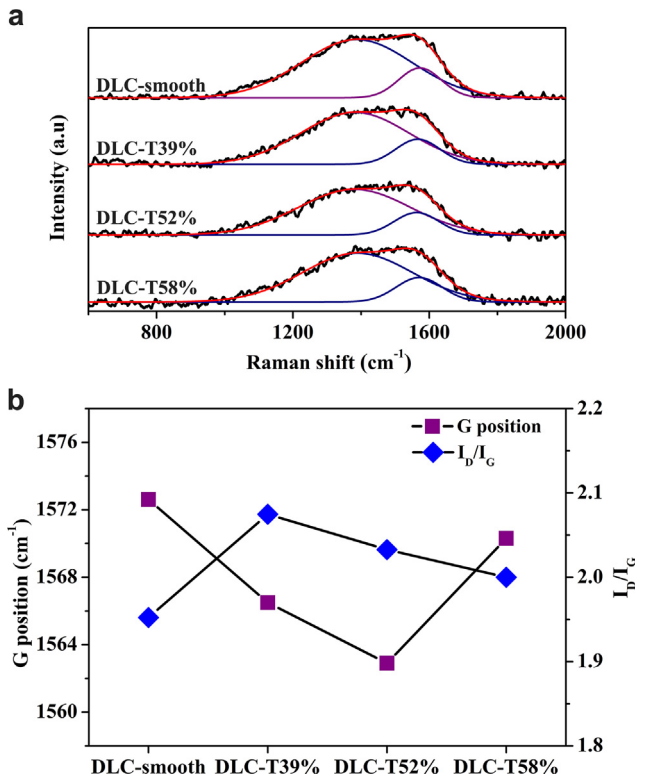

Fig. 11. Raman spectra of wear tracks (a) and the corresponding I_D/I_G and G peak position (b) under liquid lubrication condition.

Table 2
The fitting results of Raman spectra in Figs. 3 and 11a.

Samples		D peak position (cm^{-1})	G peak position (cm^{-1})	I_D/I_G
DLC-smooth	As-deposited	1377	1559	1.93
	Wear track	1387	1572	1.95
DLC-T39%	As-deposited	1382	1561	1.75
	Wear track	1381	1566	2.07
DLC-T52%	As-deposited	1383	1566	1.75
	Wear track	1380	1563	2.03
DLC-T58%	As-deposited	1384	1565	1.87
	Wear track	1389	1570	2.0

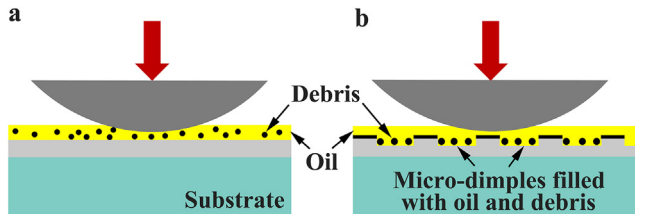

Fig. 12. Schematic illustration of friction and wear mechanism for un-textured (a) and textured specimens (b) under liquid lubrication condition.

tremendously reducing the lubricant film thickness, then deteriorating the friction and wear behavior. Therefore, the average COF and wear rate of the DLC-T58% went down to the minimum.

4. Conclusions

In this study, textured DLC films were in-situ fabricated by masking the substrate with metallic meshes during the deposition process. The tribological behaviors of un-textured and textured DLC films with different micro-dimples densities under dry friction and liquid lubrication condition were contrastively investigated. The key results are summarized and highlighted as follows:

(1) Textured DLC films with micro-dimples densities of 39%, 52% and 58% were successfully fabricated. It was extraordinary that the region covered by the metallic meshes became the concave part of the textured film, while the exposed region became the protruding part.
(2) In-situ surface texturing can significantly reduce friction and wear of DLC films both under dry friction and liquid lubrication conditions. Under dry friction, the improved tribological properties can be attributed to the friction induced graphitization of the textured layer and trapping of wear debris in micro-dimples. Under lubricated condition, the micro-dimples played the double role of wear debris and lubricating oil reservoirs, thus the graphitized textured layer on the worn surface combined with the liquid lubrication film achieved a solid-liquid duplex lubricating effect.
(3) Appropriate micro-dimples density is the key to achieve superior tribological properties. In this study, the textured DLC films with the micro-dimples density of 52% reached the lowest COF and wear rate both under dry and lubricated conditions.

CRediT authorship contribution statement

Dongqing He: Conceptualization, Methodology, Software, Investigation, Writing - original draft. **Chao He:** Resources, Writing - review & editing, Supervision, Data curation. **Wensheng Li:** Resources, Writing - review & editing, Supervision, Data curation. **Lunling Shang:** Validation, Formal analysis, Visualization, Software. **Liping Wang:** Validation, Formal analysis, Visualization. **Guangan Zhang:** Writing - review & editing.

Declaration of Competing Interest

The authors declare that they have no known competing financial interests or personal relationships that could have appeared to influence the work reported in this paper.

Acknowledgments

The authors are grateful for financial support from National Natural Science Foundation of China (51905244) and International science and technology cooperation program of China (2016YFE0111400).

References

[1] A. Götze, S. Makowski, T. Kunze, M. Hübner, H. Zellbeck, V. Weihnacht, A. Leson, E. Beyer, J.-O. Joswig, G. Seifert, G. Abrasonis, M. Posselt, J. Fassbender, W. Möller, S. Gemming, M. Krause, Tetrahedral amorphous carbon coatings for friction reduction of the valve train in internal combustion engines, Adv. Eng. Mater. 16 (2014) 1226–1233.
[2] H. Fukui, J. Okida, N. Omori, H. Moriguchi, K. Tsuda, Cutting performance of DLC coated tools in dry machining aluminum alloys, Surf. Coat. Technol. 187 (2004) 70–76.
[3] M.K. Fung, K.H. Lai, H.L. Lai, C.Y. Chan, N.B. Wong, I. Bello, C.S. Lee, S.T. Lee, Diamond-like carbon coatings applied to hard disks, Diam. Relat. Mater. 9 (2000) 815–818.
[4] A. Tibrewala, E. Peiner, R. Bandorf, S. Biehl, H. Lüthje, The piezoresistive effect in diamond-like carbon films, J. Micromech. Microeng. 17 (2007) S77.
[5] G. Dearnaley, J.H. Arps, Biomedical applications of diamond-like carbon (DLC) coatings: a review, Surf. Coat. Technol. 200 (2005) 2518–2524.
[6] A. Erdemir, C. Donnet, Tribology of diamond-like carbon films: recent progress and future prospects, J. Phys. D Appl. Phys. 39 (2006) R311–R327.
[7] K. Bewilogua, D. Hofmann, History of diamond-like carbon films — from first experiments to worldwide applications, Surf. Coat. Technol. 242 (2014) 214–225.
[8] H. Fu, X. Fan, W. Li, H. Li, Z. Cai, M. Zhu, Tribological behaviors of fluid-lubricated DLC films under sliding and fretting conditions, Appl. Surf. Sci. 459 (2018) 411–421.
[9] W. Li, X. Fan, H. Li, M. Zhu, L. Wang, Probing carbon-based composite coatings toward high vacuum lubrication application, Tribol. Int. 128 (2018) 386–396.
[10] C. Donnet, Recent progress on the tribology of doped diamond-like and carbon alloy

coatings: a review, Surf Coat. Tech. 100 (1998) 180–186.
[11] L. Qiang, K. Gao, L. Zhang, J. Wang, B. Zhang, J. Zhang, Further improving the mechanical and tribological properties of low content Ti-doped DLC film by W incorporating, Appl. Surf. Sci. 353 (2015) 522–529.
[12] W. Zhuang, X. Fan, W. Li, H. Li, L. Zhang, J. Peng, Z. Cai, J. Mo, G. Zhang, M. Zhu, Comparing space adaptability of diamond-like carbon and molybdenum disulfide films toward synergistic lubrication, Carbon 134 (2018) 163–173.
[13] D.Q. He, J.B. Pu, Z.B. Lu, L.P. Wang, G.G. Zhang, Q.J. Xue, Simultaneously achieving superior mechanical and tribological properties in WC/a-C nanomultilayers via structural design and interfacial optimization, J. Alloy. Compd. 698 (2017) 420–432.
[14] J. Pu, D. He, L. Wang, Effects of WC phase contents on the microstructure, mechanical properties and tribological behaviors of WC/a-C superlattice coatings, Appl. Surf. Sci. 357 (2015) 2039–2047.
[15] Q. Ding, L. Wang, Y. Wang, S.C. Wang, L. Hu, Q. Xue, Improved tribological behavior of DLC films under water lubrication by surface texturing, Tribol. Lett. 41 (2010) 439–449.
[16] A. Arslan, H.H. asjuki, M. Varman, M.A. Kalam, M.M. Quazi, K.A.H.A. Mahmud, M. Gulzar, M. Habibullah, Effects of texture diameter and depth on the tribological performance of DLC coating under lubricated sliding condition, Appl. Surf. Sci. 356 (2015) 1135–1149.
[17] T. Shimizu, T. Kakegawa, M. Yang, Micro-texturing of DLC thin film coatings and its tribological performance under dry sliding friction for microforming operation, Procedia Eng. 81 (2014) 1884–1889.
[18] Y. Tokuta, M. Kawaguchi, S. Sasaki, Effects of surface texture for improving friction properties of hydrogenated amorphous carbon films, Tribol. Online 11 (2016) 203–208.
[19] J. Zhan, M. Yang, Investigation on dimples distribution angle in laser texturing of cylinder-piston ring system, Tribol. Trans. 55 (2012) 693–697.
[20] X. Lu, M.M. Khonsari, An experimental investigation of dimple effect on the stribeck curve of journal bearings, Tribol. Lett. 27 (2007) 169–176.
[21] U. Pettersson, S. Jacobson, Influence of surface texture on boundary lubricated sliding contacts, Tribol. Int. 36 (2003) 857–864.
[22] U. Sudeep, N. Tandon, R.K. Pandey, Performance of lubricated rolling/sliding concentrated contacts with surface textures: a review, J. Tribol.-T. Asme 137 (2015).
[23] I. Etsion, State of the Art in Laser Surface Texturing, ASME 7th Biennial Conference on Engineering Systems Design and Analysis, 2004, pp. 585–593.
[24] U. Pettersson, S. Jacobson, Textured surfaces for improved lubrication at high pressure and low sliding speed of roller/piston in hydraulic motors, Tribol. Int. 40 (2007) 355–359.
[25] I. Etsion, State of the art in laser surface texturing, J. Tribol. 127 (2005) 248–253.
[26] S. Nakao, K. Yukimura, S. Nakano, H. Ogiso, DLC coating by HiPIMS: the influence of substrate bias voltage, IEEE Trans. Plasma Sci. 41 (2013) 1819–1829.
[27] A.H. Tan, Corrosion and tribological properties of ultra-thin DLC films with different nitrogen contents in magnetic recording media, Diam. Relat. Mater. 16 (2007) 467–472.
[28] P. Guo, Z. Geng, Z. Lu, G. Zhang, Z. Wu, Probing the lubrication mechanism of rough diamond-like carbon films against silicon nitride under water, Tribol. Int. 128 (2018) 248–259.
[29] T.W. Scharf, I.L. Singer, Role of the transfer film on the friction and wear of metal carbide reinforced amorphous carbon coatings during run-in, Tribol. Int. 36 (2009) 43–53.
[30] A.C. Ferrari, J. Robertson, Interpretation of Raman spectra of disordered and amorphous carbon, Phys. Rev. B 61 (2000) 14095–14107.
[31] C. Casiraghi, A.C. Ferrari, J. Robertson, Raman spectroscopy of hydrogenated amorphous carbons, Phys. Rev. B 72 (2005).
[32] S. Ren, S. Zheng, J. Pu, Z. Lu, G. Zhang, Study of tribological mechanisms of carbon-based coatings in antiwear additive containing lubricants under high temperature, RSC Adv. 5 (2015) 66426–66437.
[33] J.D. Schall, G.T. Gao, J.A. Harrison, Effects of adhesion and transfer film formation on the tribology of self-mated DLC contacts, J. Phys. Chem. C 114 (2010) 5321–5330.
[34] S. Ren, J. Huang, M. Cui, J. Pu, L. Wang, Improved adaptability of polyaryl-ether-ether-ketone with texture pattern and graphite-like carbon film for bio-tribological applications, Appl. Surf. Sci. 400 (2017) 24–37.
[35] D. He, S. Zheng, J. Pu, G. Zhang, L. Hu, Improving tribological properties of titanium alloys by combining laser surface texturing and diamond-like carbon film, Tribol. Int. 82 (2015) 20–27.